Path Priority Routing Protocol for Underwater Wireless Sensor Network

Olayinka O. Ogundile, *Member, IEEE*, Oluwaseyi P. Babalola, *Senior Member, IEEE*, Emmanuel O. Agboola, Olabisi M. Ogundile, and Innocent E. Davidson, *Senior Member, IEEE*

***Abstract*—Underwater wireless sensor networks (UWSNs) are rapidly expanding, enabling advancements in marine technologies like seabed excavation, seismic monitoring, and environmental monitoring. UWSNs consist of small, battery-powered devices that communicate to forward data to a base station. Due to their seabed location, replacing batteries is challenging, making energy-efficient (E-E) communication crucial to extending the network's lifespan. Many routing protocols have been developed to address the challenges of underwater communication, but balancing energy consumption while maintaining high-quality service (QoS) remains difficult, especially in large-scale UWSNs. This article introduces a path priority routing protocol (PPRP) for UWSNs, which adapts the mobile selective-path priority table (MSPT) routing protocol from terrestrial wireless sensor networks (WSNs) to underwater conditions. The PPRP prioritises paths to the base station using simple yet effective rules, reducing overall energy consumption while balancing QoS requirements. Comparative analysis with recent routing protocols show that the PPRP is a performance-efficient alternative routing protocol for UWSNs.**

***Index Terms*—Energy-balanced (E-B), energy-efficient, routing protocol, sensor nodes, underwater wireless sensor networks (UWSNs).**

I. Introduction

The OCEAN contains 96% of the water on Earth, and this water is critical for human survival since it provides natural resources, marine protection, and other advantages [1]. Because of terrestrial over-development, scientists and scholars are paying increasing attention to the oceans. Despite the wealth of resources in the ocean, ocean research and monitoring is a difficult task. Therefore, underwater sensor nodes are deployed to facilitate ocean monitoring research. The underwater sensor nodes are placed in a specific oceanic region, and the self-organizing ability of the nodes is used to transmit data to the desired destination in a concept called underwater wireless sensor network (UWSN) [1], [2].

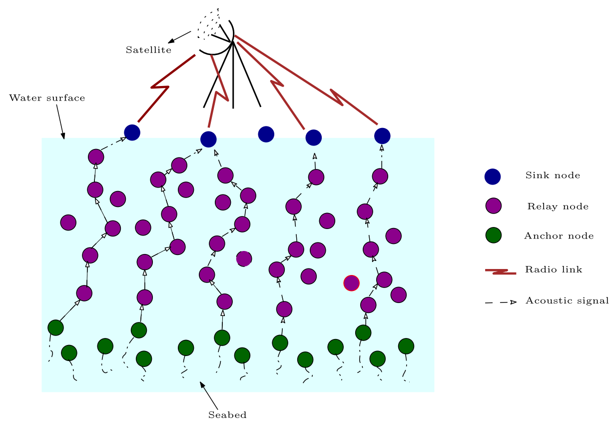

Fig. 1. Structure of a typical UWSN.

UWSN are rapidly expanding, with the potential to provide solutions to a variety of emerging marine technologies such as ocean monitoring, seismic monitoring, environmental monitoring, and seabed excavation [3], [4], [5]. UWSN is a specific application of wireless sensor network (WSN) where the sensor nodes are localised in seabed. Although they perform similar functions, UWSNs differ architecturally from terrestrial WSNs due to the properties of the communication channel (in this case, water) and the signals (acoustic waves) used to transmit the sensed data [5], [6]. Because of this communication system, the design of UWSN is quite difficult. This implies that many methods developed for terrestrial WSNs will fall short when applied to UWSNs. Therefore, to provide the best network services possible to meet the demand of UWSNs' applications, a comprehensive review of the entire network is necessary.

UWSNs comprise a group of battery powered devices called sensor nodes. They are the primary components of UWSNs and have the ability to sense and interact with one another as illustrated in Fig. 1. Routing protocol is used to identify the communication path(s) from these sensor nodes to the base station within the specified parameter of the network [7]. In particular, these routing protocols take into account the difficulties posed by the underwater media during packet forwarding and ensure that the network functions as efficiently as possible while meeting the intended objectives. Many routing protocols have been developed in the

Received 25 September 2024; revised 15 March 2025, 12 April 2025, and 2 May 2025; accepted 22 May 2025. Date of publication 27 May 2025; date of current version 25 July 2025. *(Corresponding author: Olayinka O. Ogundile.)*

Olayinka O. Ogundile is with the Department of Industrial Technical Education, Tai Solarin University of Education, Ijebu Ode 120103, Nigeria (e-mail: ogundileoo@tasued.edu.ng).

Oluwaseyi P. Babalola and Innocent E. Davidson are with the French-South African Institute of Technology, Department of Electrical, Electronic, and Computer Engineering, Cape Peninsula University of Technology, Cape Town 8000, South Africa.

Emmanuel O. Agboola is with the Department of Computing and Informatics, Bournemouth University, BH12 5BB Poole, U.K.

Olabisi M. Ogundile is with Government Senior College, Ketu-Epe, Nigeria.

Digital Object Identifier 10.1109/JIOT.2025.3574076

TABLE I
SUMMARY OF SOME EXISTING ROUTING PROTOCOLS FOR UWSNS

Routing Protocols	Design Parameters	Drawbacks
DBR [11]	D^i	Minimal depth nodes are always employed in packet transmission, leading to premature death.
EEDBR [12]	D^i, R_E	Ineffective in managing duplicate packets, especially in large-scale UWSNs.
WDFAD-DBR [8]	D^i	Minimal depth nodes are always employed in packet transmission, leading to premature death. Also ineffective in managing duplicate packets in large-scale UWSNs.
DOW-PR [9]	D^i, H_c	Nodes with low R_E are penalized, resulting in premature death.
EBER^2 [3]	D^i, R_E	Ineffective in reducing duplicate packets.
RPSOR [13]	D^i, R_E, H_c	Fails to choose a forwarder from a section with significant energy differences between neighbors.
SHEEP [5]	D^i, R_E	Does not balance energy consumption in the network, leading to void region formation.
QTAR [14]	Q-Learning, Topology Awareness	Requires extensive training and may face challenges in dynamic underwater environments.
LSTM-DQN-AM [15]	Deep Q-Network, LSTM, Adaptive Modulation	High computational requirements and potential scalability issues.
AI-Driven Routing Protocols Survey [16]	Various AI Techniques	Practical deployment is limited by hardware constraints and scalability issues despite superior performance in complex underwater environments.

literature to improve the communication in UWSNs despite the challenges imposed during underwater communication. These routing protocols, such as weighting depth and forwarding area division depth-based routing (WDFAD-DBR) [8], dolphin and whale pod routing (DOW-PR) [9], energy balanced efficient and reliable routing (EBER^2) [3], shifted energy efficiency and priority (SHEEP) [5], and so on, considered routing metrics like sensor nodes' depth information (D^i), link quality (LQ), transmission distance (T_d), hope count (H_c), and/or residual energy (R_E) in their designs. Nevertheless, balancing the energy consumption in UWSNs while meeting a high quality of service (QoS) (such as high throughput (T_p) and scalability) standard is still a challenge because of the network structure and formulation. In fact, the task of designing an energy-efficient (E-E) and energy-balanced (E-B) routing protocol becomes more challenging for large-scale UWSNs. Therefore, it is required to develop more E-E and E-B routing protocols for UWSNs to protract the network lifetime and functionality for a meaningful duration.

Consequently, this article develops a path priority routing protocol (PPRP) for UWSNs. The PPRP modifies the mobile selective-path priority table (MSPT) routing protocol proposed in [10] for terrestrial WSNs to suit UWSNs working conditions. It combines both the location-based and depth-based routing (DBR) principles in three steps: 1) Paths Identification, 2) Path Priority Matrix Formation, and 3) Path Selection. The path priority matrix is formulated based on the location information (L^i), D^i, R_E and T_d of the sensor nodes. Whereas, the PPRP selects the closest to optimal E-E path by prioritising the different paths to the sink following some uncomplicated but efficient rules. This routing approach reduces the total energy consumption (TEC) in the network while balancing other QoS requirements and functionalities. Besides, the performance of the PPRP is compared with some recent routing protocols for UWSNs such as SHEEP, EBER^2 and WDFAD-DBR in terms of the TEC, energy tax (E_{Tax}), end-to-end packet delay ($PD_{E\text{-}E}$), packet delivery ratio (PDR), and Dead/Alive nodes.

The contribution of this article is as follows. Several routing protocols have been developed in the literature to address the energy consumption challenges of UWSNs in pursuit of balancing other important QoS requirements such as T_p, scalability, timeliness, robustness, and so on. Nonetheless, the energy dissipation issue of large-scale UWSNs can be a NP-hard problem due to the network structure and formulation. In this regard, this article develops a simple but efficient routing protocol for UWSNs including large-scale. The main contribution of this article are as follows.

1) *Avoids Packet Duplication/Collision:* The proposed PPRP ensures a single E-E and E-B path is available from the source node (S_n) to the sink before a packet is forwarded. Accordingly, there are no packet duplication or retransmission that can lead to packet collision.
2) *Avoids Void Region Formation:* The proposed PPRP make sure a sensor node have sufficient battery energy before it can join the transmission chain. This implies that a sensor node will not die in the process of relaying the sensed information. Thus, it avoids void region formation for a meaningful transmission duration while increasing the PDR.
3) *E-E and E-B Routing:* The proposed PPRP offers an E-E and E-B route to the sink as it considers different routing metrics in order to select the closest to optimal path. Thus, the proposed PPRP extends the network lifetime of UWSN for a long duration, which is a major QoS requirement.

Additionally, this article will serve as a research direction for practitioners in this field and also impact the sustainability of Internet of Things (IoT) applications deployed in aquatic environments. Moreover, this contributes to advancing IoT technologies and real-world applications, particularly in underwater environmental monitoring, offshore exploration, and surveillance, where specialised protocols are essential

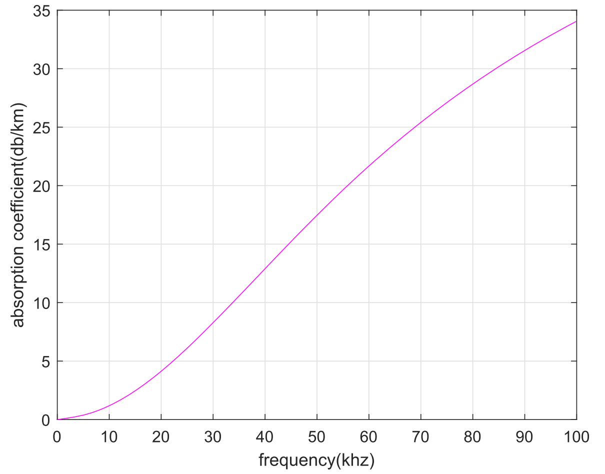

Fig. 2. Relationship between the absorption coefficient and frequency.

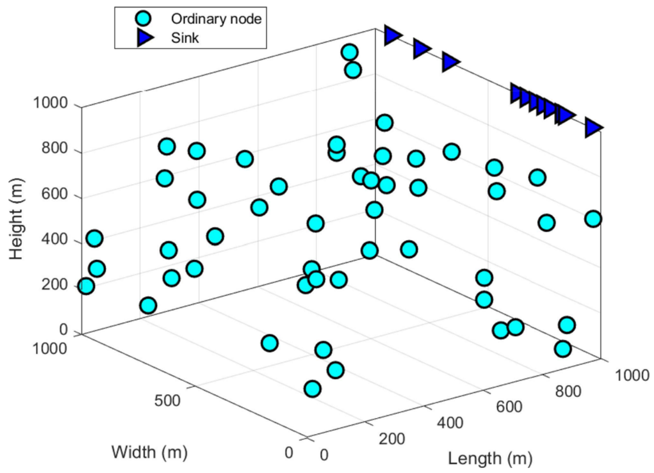

Fig. 3. USWN structure.

to overcome unique challenges posed by the underwater domain.

This article is structured as follows: Section II reviews relevant research; Section III explains the network architecture of UWSNs; Section IV discusses the proposed PPRP implementation; Section V describes the simulation setup; Section VI evaluates the performance of PPRP compared to existing protocols; and Section VII concludes with key insights.

II. Related Works

Several routing protocols have been proposed in recent years to improve the efficacy and dependability of UWSNs' communication. These routing protocols employ different design parameters in formulating their routing algorithms to avert a void region formation, limit packet duplication, and reduce the TEC in the network. The goal of these routing protocols are the same; however, their approaches somewhat differs. In [11], a DBR protocol is proposed for UWSNs. The DBR is a receiver-based algorithm that uses a greedy approach based on the sensor nodes' D^i to route packets to the sink. However, the DBR fails to balance the energy consumption in the network because the minimal depth nodes are always employed in the packet transmission, resulting in premature deaths. Yet, in [12], an E-E DBR (EEDBR) protocol was proposed for UWSNs. The EEDBR improves the performance of the DBR in terms of energy dissipation. The EEDBR combines the R_E and D^i in selecting the best path from the source node to the sink. Nevertheless, the EEDBR cannot effectively manage duplicate packets, particularly in large-scale UWSN.

Yu et al. [8] proposed a DBR algorithm termed WDFAD-DBR for UWSNs. This routing protocol is an improvement on the earlier proposed DBR. The WDFAD-DBR takes into account the weighting depth of two hops, whereas the DBR only considers the D^i of a single hop. WDFAD-DBR proactively avoids void holes by considering the depth of both the present forwarding neighbor and the projected next-hop neighbor. In the same vein, high-priority nodes are allowed to suppress low-priority nodes by dividing the forwarding area into three regions: a primary region and two subsidiary regions. The WDFAD-DBR showed some promising performance in terms of the PDR and $PD_{E\text{-}E}$ in comparison to the DBR. But, it cannot effectively manage duplicate packets and its performance plummets for large-scale UWSNs. Besides, it fails to balance the energy consumption in the network because the minimal depth nodes are always employed in the packet transmission, resulting in premature deaths.

A receiver-based routing protocol called DOW-PR was proposed in [9] for UWSNs. The authors used the D^i and H_c in choosing the next hop node toward the sink or base station. The DOW-PR reduces the TEC in the network by using nodes with smaller H_c to the sink, controlled transmission power, and choosing low traffic paths in forwarding the packets. In so doing, the DOW-PR avoids void region formation. Nevertheless, the DOW-PR does not consider the R_E of nodes. This means that the DOW-PR can select nodes low on energy to participate in the transmission round, T_{round}, resulting in premature deaths.

In [3], a receiver-based routing protocol termed EBER^2 was proposed for UWSNs. This routing protocol strives to improve the performance of the WDFAD-DBR. In achieving this, the EBER^2 takes into account the energy of the forwarding neighbor, the neighbors of the receivers, and the weighting sum of the depth difference between two hops in formulating the routing model. The EBER^2 is a heterogeneous network because it deploys two sinks underwater where there is a high density of sensor nodes. Therefore, it exhibits high PDR, E_{Tax} and $PD_{E\text{-}E}$ performances in comparison to the WDFAD-DBR. However, it cannot effectively reduce duplicate packets as in the case of the WDFAD-DBR.

A reliable path selection and opportunistic routing (RPSOR) protocol was proposed for UWSNs in [13]. The RPSOR prioritises on reliability and packet advancement in UWSNs. The next hop was selected in RPSOR by calculating three main functions; advancement factor, shortest path index, and reliability index. These function were derived based on some routing parameters such as the D^i, R_E and H_c. The RPSOR achieves better PDR, E_{Tax} and $PD_{E\text{-}E}$ performances as compared to the WDFAD-DBR. Nonetheless, the RPSOR fails to choose a forwarder from a location with significant energy differences between neighbors. Thus, it does not balance the energy consumption in the network.

An improved routing protocol called SHEEP was proposed in [5]. This routing protocol strives to solve the problems associated with the EBER^2 such as duplicate packet transmission, void region formation, and more. SHEEP considers the depth and energy of the present forwarding node, the expected next forwarding node, and the average energy difference between expected forwarders. The performance of the SHEEP surpasses the EBER^2 in terms of the TEC, E_{Tax}, $PD_{E\text{-}E}$, and PDR. Yet, the SHEEP does not efficiently balance the energy consumption in the network. For example, to prevent packet duplication, SHEEP chooses a node from a zone with the highest average energy difference among neighbors. In so doing, some particular set of nodes would be selected at all times irrespective of the T_d between the node and the sender or intended receiver. This will increase the energy consumption per node, resulting in void hole formation.

Additionally, recent research has increasingly explored the application of artificial intelligence (AI) techniques, including machine learning and fuzzy logic, to address energy efficiency challenges in UWSNs. Studies such as those by [14] and [15] have demonstrated the effectiveness of AI in optimizing energy consumption, particularly under dynamic underwater conditions [14], [15]. Furthermore, Saleem et al. [16] have reported that AI-aided routing protocols tend to outperform traditional routing approaches, especially in complex environments such as seabed terrains where conventional methods often fall short [16]. However, despite the promising performance improvements associated with AI-enhanced routing, practical implementation in real-world deployments remains constrained by several critical issues. These include hardware limitations, scalability concerns, and the overall complexity of deploying AI algorithms in underwater environments [16]. Therefore, while AI holds great potential for future UWSN routing protocols, overcoming these real-world barriers is essential for its broader adoption.

Table I provides a comprehensive summary of existing routing protocols that have been developed for UWSNs. These protocols exhibit a variety of design philosophies aimed at improving the performance and efficiency of underwater communication networks. Despite these contributions, this article introduces a novel PPRP, specifically designed for UWSNs. The proposed PPRP integrates principles from both location-based and DBR strategies. By combining these two paradigms, the PPRP seeks to minimize the TEC in the network, while maintaining a balance across other QoS requirements and critical operational functionalities.

III. Network Architecture of UWSNs

UWSNs is a subset of WSN which comprise a group of electronic battery powered devices called sensor nodes that are capable of sensing and communicating with one another without the use of any pre-existing infrastructure [17], [18]. As

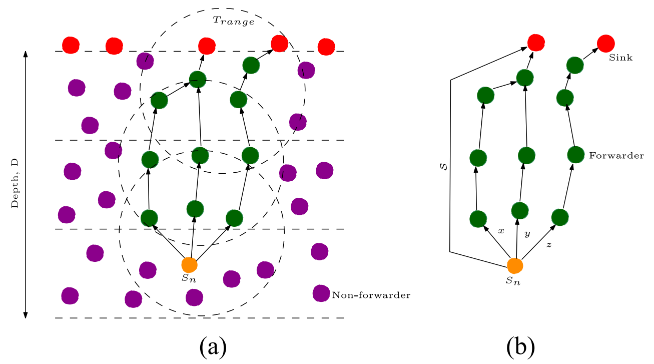

Fig. 4. Node forwarder selection.

illustrated in Fig 1, these nodes are classified into three types: 1) anchor nodes; 2) relay nodes; and 3) sink nodes [5], [19]. The anchor nodes are typically nodes that are aware of their location either by equipping them with a global positioning system or other means. They have high sensing, storage and communication ability to enable them forward packets to the upper layer nodes called relay nodes. The relay nodes serve as a bridge between the network's surface sinks and the anchor nodes in the lower layer, and are strategically placed to sense and relay all network packet. Their positions are usually not fixed because they can move with the water current [5], [20]. The sink nodes are the onshore stations that collect the data from the underwater nodes (anchor and relay nodes) and forward it to the base station. The sink nodes have both radio and acoustic modems, whereas the anchor and relay nodes only have acoustic modems. They use the embedded radio to forward the message from the anchor and relay nodes to the base station using radio links ([5], [20], [21]). As discussed in [22], underwater communication medium can be harsh and unpredictable; therefore acoustic waves are used to communicate in UWSNs. Nonetheless, researchers face different challenges using acoustic waves such as limited battery lifetime, high bit error rate, void holes, positioning and navigation problem, and packet collision/duplication [5], [23], [24], [25], [26]. Also, acoustic waves travel at almost five orders of magnitude slower than radio frequency waves, and their speed varies greatly depending on water depth, salinity, and temperature [19]. This causes lengthy propagation delays in underwater communications [19]. Furthermore, because the acoustic spectrum is limited, so is the range of useful frequencies in underwater communications [27].

A. Speed of Acoustic Channel

The propagation speed of an acoustic signal in m/s can be represented mathematically as [3], [28]

$$\begin{aligned} c = {} & 1.448.96 + 4.591T - 5.304 \times 10^{-2}T^2 + 2.374 \times 10^{-4}T^3 \\ & + 1.340(S-35) + 1.63 \times 10^{-2}D + 1.675 \times 10^{-7}D^2 \\ & - 1.025 \times 10^{-2}T(S-35) - 7.139 \times 10^{-13}D^3 \qquad (1) \end{aligned}$$

where T is the temperature in $^\circ$ C. The water temperature decreases from 22 $^\circ$ C at the top to 5 $^\circ$ C at 1 km depth, while remaining 4 $^\circ$ C below that depth. The salinity (S) is measured in parts per thousand, while the depth (D) is

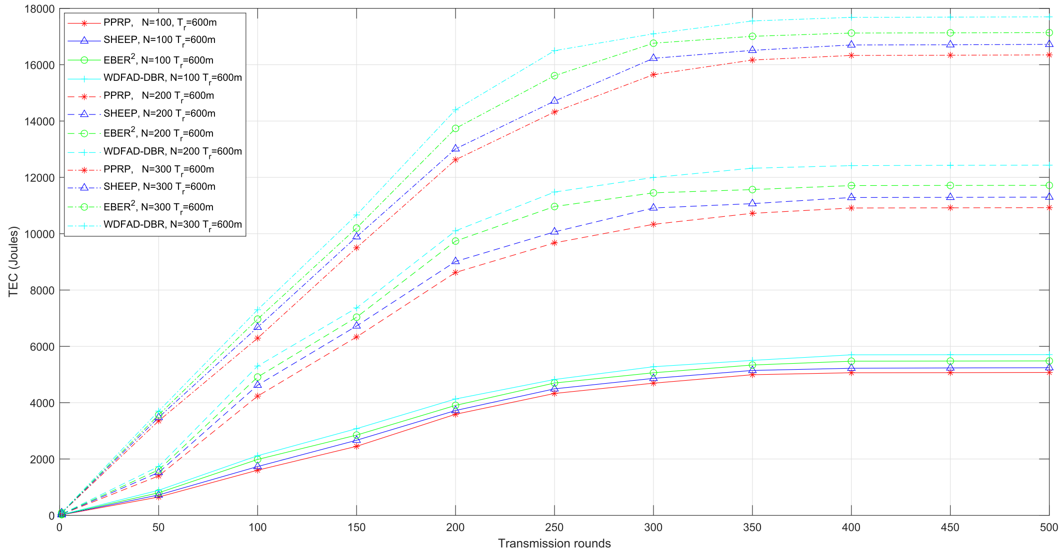

Fig. 5. TEC performance comparison; $T_r = 600$ m.

Algorithm 1 PPRP Algorithm

Input: *Sensor nodes,* L^i, D^i, R_E
Output: $\mathcal{O}_p$

Identity x, y, z and $\mathcal{S}$ *paths*
If ψ=0
Output $\mathcal{O}_p = \mathcal{S}$
Else if ψ=1
Compute 14 for the single path and $\mathcal{S}$ *path*
Output $\mathcal{O}_p$
Else
Calculate 5-10 for the multipath
Formulate the path priority table
Find $\mathcal{B}_p$ *using 11 and 12*
Compute 14 for the $\mathcal{B}_p$ *and* $\mathcal{S}$ *path*
Output $\mathcal{O}_p$
end if

TABLE II
NETWORK SIMULATION PARAMETERS

Simulation variables	Value
Deploy sensor nodes	100:50:300
Sink nodes	11
T_r	$500m$:100:$800m$
Network dimension, L	$1000m$
Network dimension, W	$1000m$
Network dimension, D	$1000m$
Transmit power	$5W$
Receive power	$0.158W$
Ideal power	$0.05W$
Frequency	$12000Hz$
Bandwidth	$4000Hz$
Propagation speed	$1500m/s$
Random walk	$3m/s$
Movement probability	0.5
Acknowledgement packet	$48bits$
Header packet	$88bits$
Payload packet	$576bits$
Request packet	$48bits$
Transmit packet	$664bits$
Data rate	$16kbps$

in meters. The acoustic sound speed rises with temperature, depth, and salinity. Eqn 1 is true when the following criteria are satisfied: $0\,^\circ$ C $\leq T \leq 30\,^\circ$ C, $0 \leq D \leq 8$ km and $30\% \leq S \leq 40\%$.

B. Energy Propagation Model

The undersea environment impacts the TEC and propagation speed of acoustic waves. The underwater communication is described using Thorp's propagation model. Acoustic channel attenuation over distance d in UWSNs can be defined as [3], [8], [29]

$$10\log A(d,f) = k \times 10\log d + d \times 10\log\alpha(f). \quad (2)$$

In (2), the first term is called the spreading loss while the second term is the called the absorption loss. The spreading coefficient k determines the propagation geometry, where k can be 1, 1.5 or 2. If $k = 1$, the spreading is cylindrical in shallow water area, $k = 1.5$, the spreading is practical, and $k = 2$, the spreading is spherical in deep water area as assumed in this article. The absorption coefficient is represented as $\alpha(f)$. Fig. 2 shows the relationship between the absorption coefficient and frequency based on Thorp's model.

The noise in an underwater environment is defined as [3], [8], [30]

$$N(f) = N_t(f) + N_s(f) + N_w(f) + N_{th}(f) \quad (3)$$

where $N_t(f)$ is the turbulence noise, $N_s(f)$ is the shipping noise, $N_w(f)$ is the waves noise and $N_{th}(f)$ is the thermal noise.

The signal-to-noise ratio (SNR) at receivers for an acoustic signal in an underwater environment with a frequency of f and a propagation distance of d can be defined as [3], [8]

$$\mathrm{SNR}(f,d) = P(f) - A(d,f) - N(f) + D_I \quad (4)$$

where the transmission power is denoted as $P(f)$, the attenuation noise is denoted as $A(d,f)$ and D_I is the directivity index. The D_I represents the ability of the sensor nodes to direct its hydrophone in order to prevent unwanted noise.

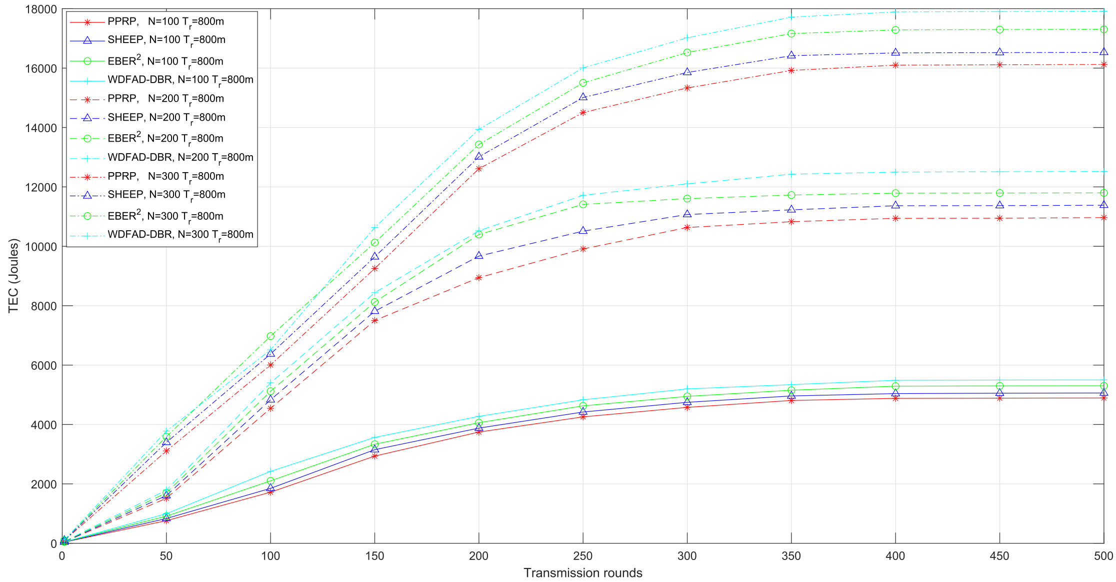

Fig. 6. TEC performance comparison; $T_r = 800$ m.

TABLE III
TEC PERFORMANCE COMPARISON; $T_r = 600$ M

$N = 100$

Routing protocol	T_{round} 1	50	100	150	200	250	300	350	400	450	500
PPRP	17.8	649.4	1602.7	2449.9	3588.7	4327.2	4692.3	4992.2	5062.2	5066.2	5073.2
SHEEP	20.1	722.8	1732.2	2666.1	3721.9	4491.2	4862.5	5144.4	5222.2	5233.2	5241.2
$EBER^2$	23.0	800.3	1984.5	2848.5	3903.6	4697.9	5061.8	5337.3	5472.7	5478.3	5482.4
WDFAD-DBR	25.9	889.9	2116.8	3077.7	4131.5	4823.1	5276.5	5501.2	5699.1	5701.9	5706.3

$N = 200$

Routing protocol	T_{round} 1	50	100	150	200	250	300	350	400	450	500
PPRP	37.9	1399.0	4232.8	6333.5	8623.6	9674.4	10332.9	10723.8	10912.4	10919.3	10924.7
SHEEP	40.2	1522.1	4620.6	6723.6	9012.4	10063.7	10913.4	11067.4	11284.7	11289.4	11298.9
$EBER^2$	44.3	1614.4	4909.4	7034.8	9738.5	10964.9	11450.2	11566.5	11708.6	11713.7	11716.3
WDFAD-DBR	48.8	1733.7	5299.6	7363.7	10101.7	11478.3	11996.3	12325.6	12416.9	12428.1	12433.6

$N = 300$

Routing protocol	T_{round} 1	50	100	150	200	250	300	350	400	450	500
PPRP	89.7	3353.4	6291.3	9500.2	12624.6	14320.2	15647.5	16166.4	16329.1	16337.5	16348.6
SHEEP	91.5	3476.6	6678.9	9889.8	13012.3	14708.9	16227.8	16510.1	16701.3	16707.6	16722.5
$EBER^2$	95.3	3568.2	6966.7	10200.4	13738.3	15609.6	16763.8	17008.7	17124.9	17131.8	17139.1
WDFAD-DBR	100.1	3701.1	7299.9	10666.6	14398.5	16498.3	17097.4	17553.8	17681.1	17689.7	17699.6

IV. PROPOSED PPRP

A. MSPT: Rational for Design Modification

The existing MSPT proposed for terrestrial WSNs in [10] is a clustering E-E and E-B routing protocol. The routing protocol prioritises the best path to the sink based on some routing metrics. It selects two multipath ($\psi = 2$) to the sink using multihop communication and a straight (direct) path, totalling up to three paths. It then selects the one that is closest to optimal among these paths. The MSPT performs well in contrast to other terrestrial routing protocol in the literature. Nevertheless, it is not suitable for UWSNs working conditions. The main reason for MSPT failure in UWSNs is node localization. As shown in Fig. 3, sensor nodes in UWSNs are in a 3-D space (length, width, and depth) and the position of some nodes change continuously due to the water current. Whereas, in terrestrial WSN, nodes are in 2-D space (length and width), and the positions of the nodes are fixed. In MSPT, the network structure considers only the L and W (length and width) coordinates in calculating the distance between two nodes. Such an approach will fail in UWSN, because the depth is pivotal in selecting the next forwarder node. Thus, this proposed PPRP incorporates the D^i in selecting the next forwarder node.

Also, to improve routing performance; most especially, because UWSNs use more sink node, the number of multipath is raised to $\psi = 3$, which can be further increased based on the network size, N. This increase is because there are more sink nodes in the network compared to the single one in the network assumptions for the MSPT. This implies that the

TABLE IV
TEC PERFORMANCE COMPARISON; $T_r = 800$ M

$N = 100$

Routing protocol	T_{round} 1	50	100	150	200	250	300	350	400	450	500
PPRP	38.9	761.3	1720.3	2935.7	3745.0	4256.5	4576.5	4808.7	4880.0	4887.4	4892.3
SHEEP	41.2	834.7	1849.8	3151.9	3878.2	4420.5	4746.7	4960.9	5040.0	5054.4	5060.3
$EBER^2$	44.1	912.2	2102.1	3334.3	4059.9	4627.2	4946.0	5153.8	5290.5	5299.5	5301.5
WDFAD-DBR	46.9	996.4	2421.7	3565.6	4273.4	4831.5	5198.1	5342.3	5488.8	5496.9	5499.8

$N = 200$

Routing protocol	T_{round} 1	50	100	150	200	250	300	350	400	450	500
PPRP	48.1	1515.3	4543.6	7501.7	8944.4	9909.9	10633.2	10828.1	10942.4	10945.3	10965.7
SHEEP	52.2	1607.6	4831.4	7812.6	9670.6	10510.1	11069.7	11227.5	11365.8	11369.4	11382.3
$EBER^2$	56.4	1698.9	5119.3	8123.7	10396.4	11411.3	11606.2	11725.9	11789.4	11793.5	11799.1
WDFAD-DBR	60.8	1792.2	5401.0	8437.9	10523.4	11717.8	12102.6	12428.2	12498.8	12510.2	12519.9

$N = 300$

Routing protocol	T_{round} 1	50	100	150	200	250	300	350	400	450	500
PPRP	95.7	3109.9	6004.4	9253.7	12612.1	14503.3	15332.3	15922.3	16100.2	16111.5	16123.2
SHEEP	98.2	3397.7	6373.3	9644.4	13011.9	15010.0	15852.6	16417.5	16512.4	16522.2	16531.3
$EBER^2$	104.3	3589.3	6975.8	10124.3	13427.4	15503.6	16525.8	17163.8	17286.3	17297.4	17305.5
WDFAD-DBR	111.1	3776.7	6512.6	10633.3	13938.9	16006.8	17019.9	17717.5	17891.8	17902.2	17913.1

identified paths may be forwarding to different sinks as shown in Fig. 4. Therefore, with more sinks, there can be more E-E and E-B paths from the S_n, promoting optimum path selection.

B. PPRP Network Assumptions

Fig. 3 shows the typical structure of an UWSN with N_o ordinary nodes and N_s sinks distributed nonuniformly to sense the underwater environment. Note that the sensor nodes are not clustered as in the MSPT. The following basic assumptions are made concerning this UWSN.

1) The network is homogeneous.
2) Sensor nodes are aware of their location as well as the locations of their neighbors; that is L^i.
3) Sensor nodes are aware of their depth as well as the depths of their neighbors; that is D^i.
4) Sensor nodes are aware of their neighbors' R_E.
5) The sensor nodes have a fixed transmission range (T_r) and cannot transmit beyond the value of T_r.
6) The sensor nodes have their unique ID to adapt to any security architecture.
7) Sensor nodes are not clustered, and every node forwards their message to the sink directly or via multihop communications.

C. PPRP Implementation

The PPRP operates in three phases: 1) Paths identification, 2) Path priority matrix formation, and 3) Path selection. The paths identification phase entails identifying several potential E-E routes to the nearest sink. The second phase creates a path matrix for these identified E-E paths in the first phase, and the final phase uses the path priority matrix to select the most E-E and E-B path to the sink among these identified paths.

1) Paths Identification: Consider the simplified UWSN of Fig. 4(a), where the S_n attempts to forward its sensed information to the nearest sink using the most E-E and E-B route. The S_n selects $\psi = 3$ nearest nodes within its T_r and toward the sink based on their L^i and D^i. Afterwards, these forwarder nodes select the nearest node within their T_r toward the sink. The process continues until $\psi = 3$ paths are formed to the sink. Likewise, the S_n selects a straight ($\mathcal{S}$) path to the sink, totalling up to four paths as shown in Fig. 4(b).

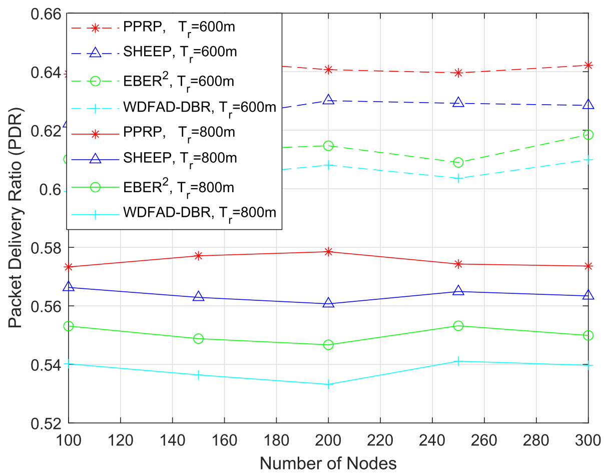

Fig. 7. PDR performance comparison for different N; $T_{\text{round}} = 100$.

In Fig. 4(b), x, y and z represent the $\psi = 3$ paths to the sink while $\mathcal{S}$ represents the straight path. Notably, regardless of the T_d, the S_n only chooses a node as the forwarder node if its R_E is at least 50% of its own. Likewise, the next forwarder nodes select their respective receiver using the same condition. If S_n is close to the sink, there may be fewer than $\psi = 3$ paths, and the $\mathcal{S}$ path. That is, $\psi < 3$ paths and the $\mathcal{S}$ path. In some rare circumstances; most especially as the T_{round} increases, there

TABLE V
PDR PERFORMANCE COMPARISON FOR DIFFERENT N; $T_{Round} = 100$

$T_r = 600m$

Routing protocol	N = 100	150	200	250	300
PPRP	0.6392	0.6439	0.6407	0.6396	0.6422
SHEEP	0.6222	0.6232	0.6301	0.6292	0.6285
$EBER^2$	0.6101	0.6131	0.6147	0.6090	0.6185
WDFAD-DBR	0.5991	0.6038	0.6081	0.6036	0.6099

$T_r = 800m$

Routing protocol	N = 100	150	200	250	300
PPRP	0.5733	0.5771	0.5785	0.5743	0.5736
SHEEP	0.5663	0.5629	0.5607	0.5649	0.5634
$EBER^2$	0.5531	0.5488	0.5467	0.5532	0.5499
WDFAD-DBR	0.5402	0.5364	0.5332	0.5411	0.5397

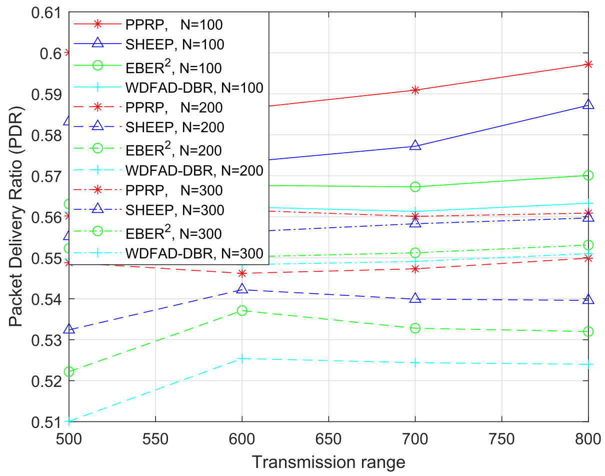

Fig. 8. PDR performance comparison for different T_r; $T_{\text{round}} = 100$.

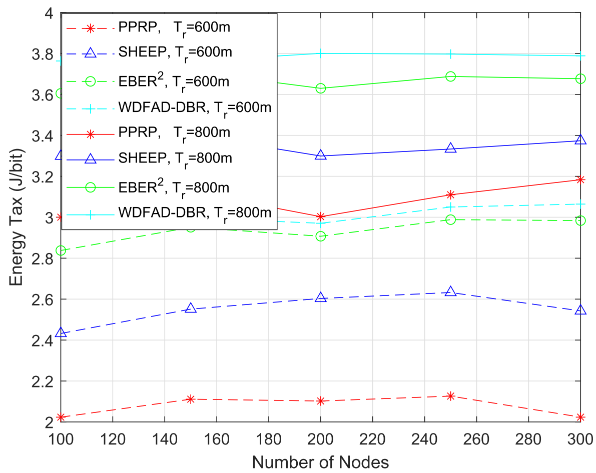

Fig. 9. E_{Tax} performance comparison for different N; $T_{\text{round}} = 100$.

may be no other route to the sink except through the $\mathcal{S}$ path. Thus, the S_n forwards the message directly to the sink.

2) Path Priority Matrix Formation: The PPRP creates a path priority matrix following the paths identification. The path priority matrix, which shows the energy cost of each identified path is formulated based on the following routing metrics.

TABLE VI
PDR PERFORMANCE COMPARISON FOR DIFFERENT T_r; $T_{\text{round}} = 100$

$N = 100$

Routing protocol	T_r = $500m$	$600m$	$700m$	$800m$
PPRP	0.6001	0.5863	0.5909	0.5972
SHEEP	0.5832	0.5733	0.5772	0.5872
$EBER^2$	0.5631	0.5677	0.5673	0.5701
WDFAD-DBR	0.5611	0.5624	0.5613	0.5633

$N = 200$

Routing protocol	T_r = $500m$	$600m$	$700m$	$800m$
PPRP	0.5488	0.5462	0.5473	0.5499
SHEEP	0.5324	0.5422	0.5399	0.5396
$EBER^2$	0.5222	0.5371	0.5328	0.5320
WDFAD-DBR	0.5101	0.5254	0.5244	0.5240

$N = 300$

RPs	TR = $500m$	$600m$	$700m$	$800m$
PPRP	0.5602	0.5616	0.5601	0.5609
SHEEP	0.5552	0.5563	0.5583	0.5597
$EBER^2$	0.5523	0.5502	0.5512	0.5531
WDFAD-DBR	0.5497	0.5483	0.5491	0.5510

TABLE VII
E_{Tax} PERFORMANCE COMPARISON FOR DIFFERENT N; $T_{\text{round}} = 100$

$T_r = 600m$

Routing protocol	N = 100	150	200	250	300
PPRP	2.0233	2.1111	2.1022	2.1262	2.0234
SHEEP	2.4322	2.5512	2.6033	2.6323	2.5424
$EBER^2$	2.8376	2.9511	2.9072	2.9883	2.9837
WDFAD-DBR	2.9998	2.9967	2.9706	3.0501	3.0643

$T_r = 800m$

Routing protocol	N = 100	150	200	250	300
PPRP	3.0003	3.1242	3.0028	3.1098	3.1834
SHEEP	3.2983	3.4024	3.2992	3.3333	3.3738
$EBER^2$	3.6053	3.7115	3.6299	3.6879	3.6768
WDFAD-DBR	3.7635	3.7622	3.8006	3.7971	3.7886

1) *Total Energy, T_{energy}:* The PPRP calculates the TEC for each path to forward the sensed information to the sink. The T_{energy} is the total energy consumed in transmitting the sensed information to the sink from the S_n. Mathematically, it is given as

$$T_{\text{energy}} = \sum_{1}^{\lambda} \mathcal{E}_\lambda \tag{5}$$

where λ is the number of participating nodes in forwarding the information to the sink and $\mathcal{E}_\lambda$ is the energy consumed by each node including the S_n. In the case of the $\mathcal{S}$ path, $\lambda = 1$ because there are no intermediate node. A small value of T_{energy} is desirable always as it indicates an E-E path to the sink. However, this is not the case if critically analysed. For example, a node in that chain might dissipates twice as much energy as the other node in the relay chain. This indicates that the energy expended in that path is not uniformly distributed, and that some nodes may die over time, resulting in void

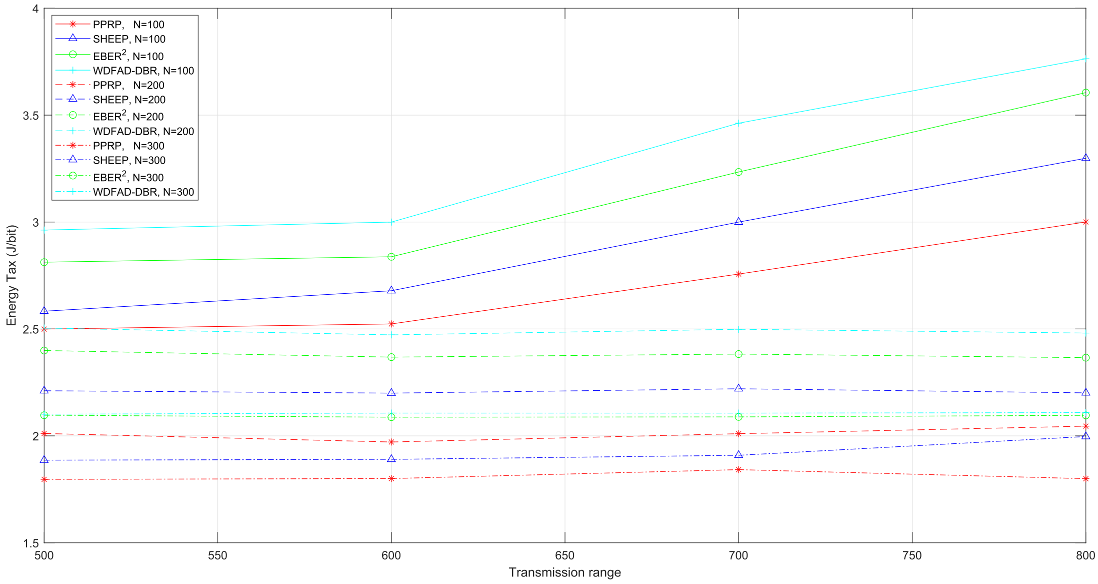

Fig. 10. E_{Tax} performance comparison for different T_r; $T_{\text{round}} = 100$.

TABLE VIII
E_{Tax} PERFORMANCE COMPARISON FOR DIFFERENT T_r; $T_{\text{round}} = 100$

$N = 100$

Routing protocol	T_r 500m	600m	700m	800m
PPRP	2.4993	2.5234	2.7567	3.0003
SHEEP	2.5829	2.6787	2.9998	3.2983
$EBER^2$	2.8123	2.8376	3.2341	3.6053
WDFAD-DBR	2.9625	2.9998	3.4623	3.7635

$N = 200$

Routing protocol	T_r 500m	600m	700m	800m
PPRP	2.0111	1.9713	2.0101	2.0453
SHEEP	2.2109	2.1999	2.2202	2.2011
$EBER^2$	2.3991	2.3682	2.3825	2.3656
WDFAD-DBR	2.5042	2.4723	2.4984	2.4808

$N = 300$

Routing protocol	T_r 500m	600m	700m	800m
PPRP	1.7965	1.8004	1.8421	1.7998
SHEEP	1.8864	1.8901	1.9091	1.9969
$EBER^2$	2.0964	2.0874	2.0887	2.0958
WDFAD-DBR	2.1014	2.1066	2.1064	2.1087

region formation. Accordingly, more features are added to the path priority matrix to monitor such situations.

2) *Energy Range, E_{range}:* The E_{range} ensures there is a balance in the energy dissipated among the nodes in that chain. It is expressed as

$$E_{\text{range}} = \max(E_\gamma) - \min(E_\gamma) \quad (6)$$
$$E_\gamma = [\mathcal{E}_1 \ \mathcal{E}_2 \ \cdots \ \mathcal{E}_\lambda]'. \quad (7)$$

A minimal E_{range} value indicates an evenly dispersed energy dissipation along the path. The E_{range} value is not computed for the $\mathcal{S}$ route because it is single-hop communication; thus, E_{range} is always equal to zero.

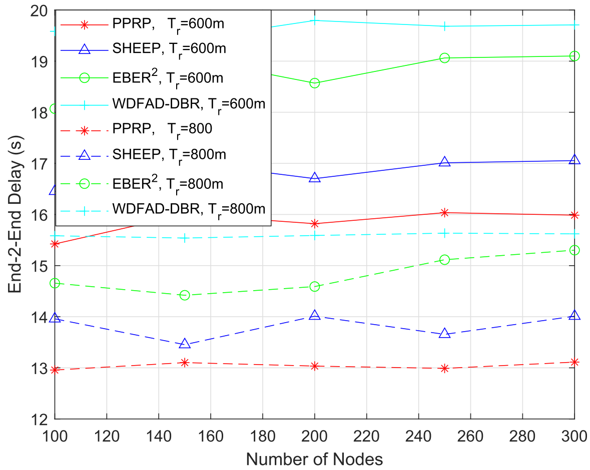

Fig. 11. End-to-end packet delay performance comparison; $T_{\text{round}} = 100$.

3) *Energy Ratio, E_{ratio}:* The E_{ratio} is also used to balance the energy dissipated in the network. It is expressed as

$$E_{\text{ratio}} = \frac{\max(E_\gamma)}{\sum_1^\lambda \mathcal{E}_\lambda}. \quad (8)$$

Similar to E_{range} and T_{energy}, a small E_{ratio} value is appropriate because it shows a balance in network energy consumption. The E_{ratio} for the $\mathcal{S}$ route is always equal to one, hence it is not computed.

4) *Energy Percentage, $E_{percentage}$:* The $E_{\text{percentage}}$ measures the proportion of energy dissipated by the sensor nodes in a path, with the maximum recorded in the path priority matrix for each path. It is expressed as

$$E_{\text{percentage}} = \max(E_\sigma) \quad (9)$$
$$E_\sigma = \left[\frac{\mathcal{E}_1}{R_{E_1}}\% \ \frac{\mathcal{E}_2}{R_{E_2}}\% \ \cdots \ \frac{\mathcal{E}_\lambda}{R_{E_\lambda}}\%\right]' \quad (10)$$

TABLE IX
END-TO-END PACKET DELAY PERFORMANCE COMPARISON; $T_{\text{round}} = 100$

$T_r = 600m$

Routing protocol	N				
	100	150	200	250	300
PPRP	$15.4235s$	$16.0001s$	$15.8201s$	$16.0358s$	$15.9867s$
SHEEP	$16.4526s$	$17.0220s$	$16.7013s$	$17.0111s$	$17.0542s$
$EBER^2$	$18.0697s$	$19.0650s$	$18.5700s$	$19.0623s$	$19.1007s$
WDFAD-DBR	$19.5835s$	$19.4150s$	$19.7957s$	$19.6823s$	$19.7092s$

$T_r = 800m$

Routing protocol	N				
	100	150	200	250	300
PPRP	$12.9567s$	$13.1023s$	$13.0342s$	$12.9889s$	$13.1123s$
SHEEP	$13.9589s$	$13.4532s$	$14.0100s$	$13.6551s$	$14.0101s$
$EBER^2$	$14.6563s$	$14.4200s$	$14.5900s$	$15.1150s$	$15.3021s$
WDFAD-DBR	$15.5835s$	$15.5392s$	$15.5893s$	$15.6345s$	$15.6211s$

where R_{E_λ} is the residual energy of the λth node before attempting to forward the message. The $E_{\text{percentage}}$ ensures that all the nodes in the path can still participate in subsequent data T_{round}. A small value of the $E_{\text{percentage}}$ indicates that the energy consumption along that path is balanced.

3) Path Selection: Following the formation of the path priority matrix, the entries are ranked to determine the best path, $\mathcal{B}_p$ from the S_n to the sink among the $\psi = \lambda$ paths. First, the $\psi = \lambda$ paths to the sink are given a priority ranking. Equation 11 shows the simple matrix representation of the multipath

$$E_\chi = \begin{bmatrix} \overbrace{P_{1,1}}^{x} & \overbrace{P_{1,2}}^{y} & \overbrace{P_{1,\lambda}}^{z} \\ P_{2,1} & P_{2,2} & P_{2,\lambda} \\ P_{3,1} & P_{3,2} & P_{3,\lambda} \\ P_{4,1} & P_{4,2} & P_{4,\lambda} \end{bmatrix} \tag{11}$$

where the elements in row 1 of E_χ represent the T_{energy} for the x, y, and z paths. Similarly, rows 2, 3, and 4 of E_χ represent the E_{range}, E_{ratio}, and $E_{\text{percentage}}$ routing metrics, respectively. As explained in Section IV-C2, a low value of the four metrics indicate an E-E path. Therefore, the path with the highest proportion of the least value of these four metrics is chosen as the $\mathcal{B}_p$. This can be expressed as

$$\mathcal{B}_p = \text{mode}\begin{bmatrix} \min(P_{1,1}\ P_{1,2}\ P_{1,\lambda}) \\ \min(P_{2,1}\ P_{2,2}\ P_{2,\lambda}) \\ \min(P_{3,1}\ P_{3,2}\ P_{3,\lambda}) \\ \min(P_{4,1}\ P_{4,2}\ P_{4,\lambda}) \end{bmatrix}. \tag{12}$$

From the simulation runs, it is observed that in some rare cases, two paths have equal proportion of the least value of these four metrics. As such, the path that has the lowest T_{energy} is selected as the $\mathcal{B}_p$. Finally, the $\mathcal{B}_p$ is compared to the $\mathcal{S}$ path. While T_{energy} and $E_{\text{percentage}}$ are calculated for the $\mathcal{S}$ path, $E_{\text{percentage}}$ is the sole metric used for comparison with the $\mathcal{B}_p$. The $\mathcal{S}$ path often has the lowest T_{energy} in comparison to the x, y, and z paths; however, it may not be the most E-E path. To ensure fair comparison, only the $E_{\text{percentage}}$ routing metric is used.

Thus, the path to the nearest sink from the S_n is selected between the $\mathcal{B}_p$ and $\mathcal{S}$ path based on their $E_{\text{percentage}}$ as

$$\mathcal{O}_p = \min\big(E_\rho\big) \tag{13}$$

$$E_\rho = \big[E_{\text{percentage}}(\mathcal{S}), E_{\text{percentage}}\big(\mathcal{B}_p\big)\big] \tag{14}$$

where $E_{\text{percentage}}(\mathcal{S})$ and $E_{\text{percentage}}(\mathcal{B}_p)$ are the $E_{\text{percentage}}$ of the $\mathcal{B}_p$ and $\mathcal{S}$ path, respectively. In cases where there is only one path and the $\mathcal{S}$ path, the routing protocol calculates the $E_{\text{percentage}}$ for these paths to select the $\mathcal{O}_p$. The PPRP routing steps is summarised in Algorithm 1.

V. SIMULATION SET-UP

In the set-up, a 3-D space of $L = 1000$, $W = 1000$ m, and $D = 1000$ m is considered as shown in Fig. 5. The number of sensor nodes, N are varied from 100 to 300, in intervals of 50 to verify the performance of the proposed PPRP for scalability. The T_r of the sensor nodes are also varied from 500 to 800 m in steps of 100 m to document the performance of the proposed PPRP for different transmission distances. Most of the sensor nodes are deployed randomly underwater except for the anchor nodes which are deployed at the bottom of the sea. Likewise, the sink nodes are deployed randomly at the surface of the water to forward the message from the anchor and relay nodes to the base station. Each node in the network is equipped with a battery energy of $60J$. The transmit, receive, and ideal powers are set to 5, 0.158, and 0.05 W, respectively. The packet sizes for acknowledgement, header, payload, request, and transmit are given as $48bits$, $88bits$, $576bits$, $48bits$, and $664bits$, respectively. The network simulation takes into account an acoustic propagation speed of 1500 m/s and a data rate of 16 kb/s. More so, the network assumes dynamic nodes drift, where the relay nodes can only move left or right with a moving probability of 0.5 and a speed of 3 m/s. Table II summarises the deployed parameters.

VI. PERFORMANCE EVALUATION OF PROPOSED PPRP

The proposed PPRP is compared with the existing SHEEP and EBER^2 routing protocols for five different performance metrics; TEC, PDR E_{Tax}, $PD_{E\text{-}E}$ and dead/alive nodes.

A. TEC

Figs. 5 and 6 illustrate the TEC versus T_{round} performance of the proposed PPRP for $T_r = 600$ m and $T_r = 600$ m, respectively. First, the figures show that the TEC increases

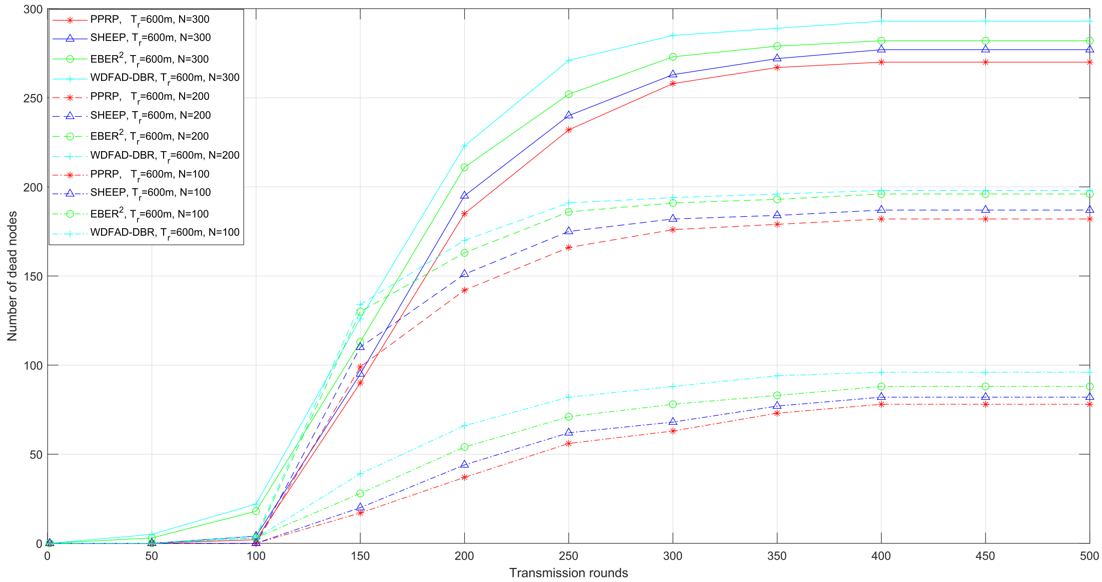

Fig. 12. Dead nodes versus T_{round}, $T_r = 600$ m.

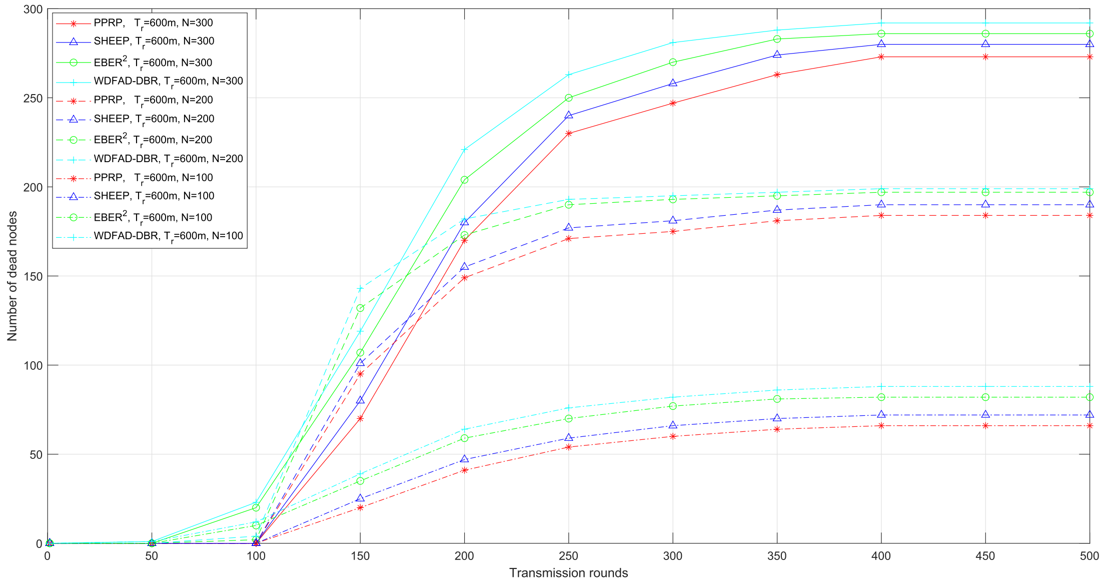

Fig. 13. Dead nodes versus T_{round}, $T_r = 800$ m.

with the T_{round}, even when the T_r increases from 600 to 800 m. Second, the proposed PPRP outperforms the SHEEP, EBER^2, and WDFAD-DBR routing protocols in both figures, since it dissipates the least battery energy in conveying the message to the base station. This is because the PPRP is an E-E and E-B routing protocol that balances the energy consumption at every T_{round} by picking the optimal path to the nearest sink from the S_n based on four reliable routing metrics. To buttress, Tables III and IV, show the TEC values of the SHEEP, EBER^2 and WDFAD-DBR routing protocols, as the network grows in size. Note the robustness in the performance of the PPRP as compared to the SHEEP, EBER^2 and WDFAD-DBR routing protocols, even when T_r increases from 600 to 800 m.

B. PDR

The PDR is the ratio of the total packets delivered to the total packets sent from source to destination nodes [13], [31]. It is given as

$$\text{PDR} = \frac{\sum \text{Total packet received}}{\sum \text{Total packet transmitted}}. \quad (15)$$

The PDR performance of the proposed PPRP are shown in Figs. 7 and 8 for $T_{\text{round}} = 100$. In Fig 7, the PDR performance is examined for various N. As shown, the PDR performance of the PPRP surpasses the SHEEP, EBER^2, and WDFAD-DBR routing protocols, even as the network expands in size. This is because the energy consumed in the network is low while using the proposed PPRP routing protocol in contrast

TABLE X
DEAD NODES VERSUS T_{round}, $T_r = 600$ M

$N = 100$

	T_{round}										
Routing protocol	1	50	100	150	200	250	300	350	400	450	500
PPRP	0	0	0	17	37	56	63	73	78	78	78
SHEEP	0	0	0	20	44	62	68	77	82	82	82
$EBER^2$	0	0	3	28	54	71	78	83	88	88	88
WDFAD-DBR	0	0	3	39	66	82	88	94	96	96	96

$N = 200$

	T_{round}										
Routing protocol	1	50	100	150	200	250	300	350	400	450	500
PPRP	0	0	0	99	142	166	176	179	182	182	182
SHEEP	0	0	0	110	151	175	182	184	187	187	187
$EBER^2$	0	0	3	130	163	186	191	193	196	196	196
WDFAD-DBR	0	0	4	134	170	191	194	196	198	198	198

$N = 300$

	T_{round}										
Routing protocol	1	50	100	150	200	250	300	350	400	450	500
PPRP	0	0	2	90	185	232	258	267	270	270	270
SHEEP	0	0	4	95	195	240	263	272	277	277	277
$EBER^2$	0	3	18	113	211	252	273	279	282	282	282
WDFAD-DBR	0	5	22	126	223	271	285	289	293	293	293

TABLE XI
DEAD NODES VERSUS T_{round}, $T_r = 800$ M

$N = 100$

	T_{round}										
Routing protocol	1	50	100	150	200	250	300	350	400	450	500
PPRP	0	0	0	70	170	230	247	263	273	273	273
$EBER^2$	0	0	0	80	180	240	258	274	280	280	280
SHEEP	0	0	20	107	204	250	270	283	286	286	286
WDFAD-DBR	0	1	23	119	221	263	281	288	292	292	292

$N = 200$

	T_{round}										
Routing protocol	1	50	100	150	200	250	300	350	400	450	500
PPRP	0	0	0	95	149	171	175	181	184	184	184
SHEEP	0	0	0	101	155	177	181	187	190	190	190
$EBER^2$	0	0	2	132	173	190	193	195	197	197	197
WDFAD-DBR	0	0	4	143	182	193	195	197	199	199	199

$N = 300$

	T_{round}										
Routing protocol	1	50	100	150	200	250	300	350	400	450	500
PPRP	0	0	0	70	170	230	247	263	273	273	273
SHEEP	0	0	0	80	180	240	258	274	280	280	280
$EBER^2$	0	0	20	107	204	250	270	283	286	286	286
WDFAD-DBR	0	1	23	119	221	263	281	288	292	292	292

to the SHEEP, EBER^2 and WDFAD-DBR routing protocols. As a result, the sensor nodes' lifetime is extended for an acceptable amount of time, allowing them to send more data to the base station. To emphasize, Table V shows the numerical results of the PPRP in comparison to the other routing protocols. It can be clearly seen from the table that the PPRP offered the best PDR performance, even as T_r increase from 600 to 800 m. Likewise, Fig 8 shows the superior PDR performance of the PPRP over the SHEEP, EBER^2, and WDFAD-DBR routing protocols as T_r increases. To buttress, Table VI shows that the PPRP has a higher PDR value than the SHEEP, EBER^2, and WDFAD-DBR routing protocols as the network grows, demonstrating that the PPRP is scalable.

C. E_{Tax} Performance

The E_{Tax} is the TEC per node in forwarding a packet from the source node to the destination node [5], [32]. It is expressed mathematically as

$$E_{\text{Tax}} = \frac{\text{TEC}}{\text{number of nodes} \times \text{packet size}}. \quad (16)$$

Figs. 9 and 10 show the E_{Tax} performance of the PPRP for increasing N and T_r, respectively, assuming $T_{\text{round}} = 100$. As noted in Fig 9, the PPRP has the lowest E_{Tax} in comparison to the SHEEP, EBER^2, and WDFAD-DBR routing protocols, even as the network grows in size. This is because the PPRP prevents packet collisions, allowing for additional packets to be transmitted to the base station. Whereas, (16) demonstrates

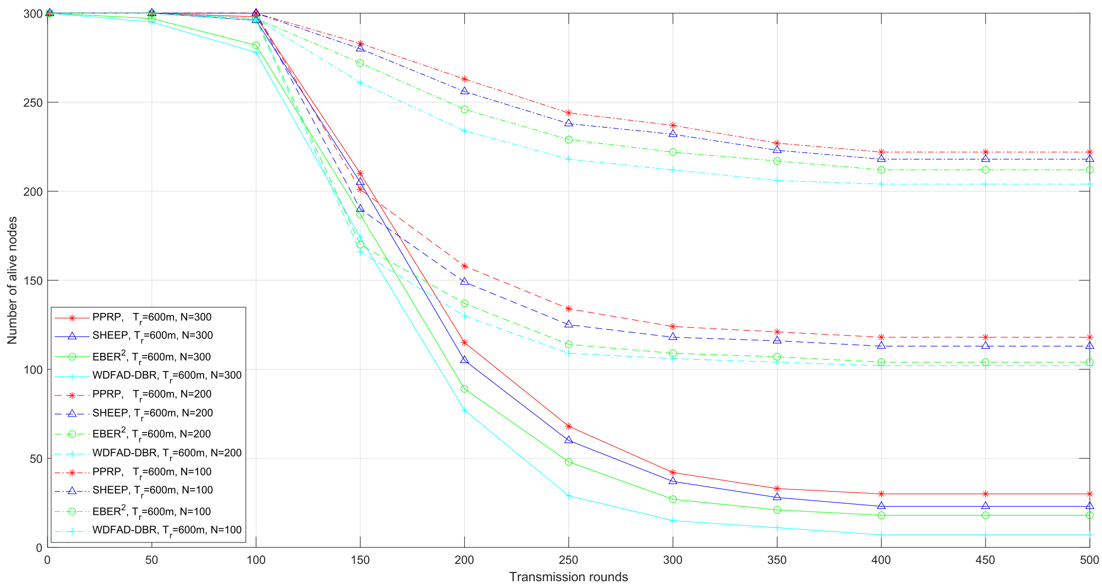

Fig. 14. Alive nodes versus T_{round}, $T_r = 600$ m.

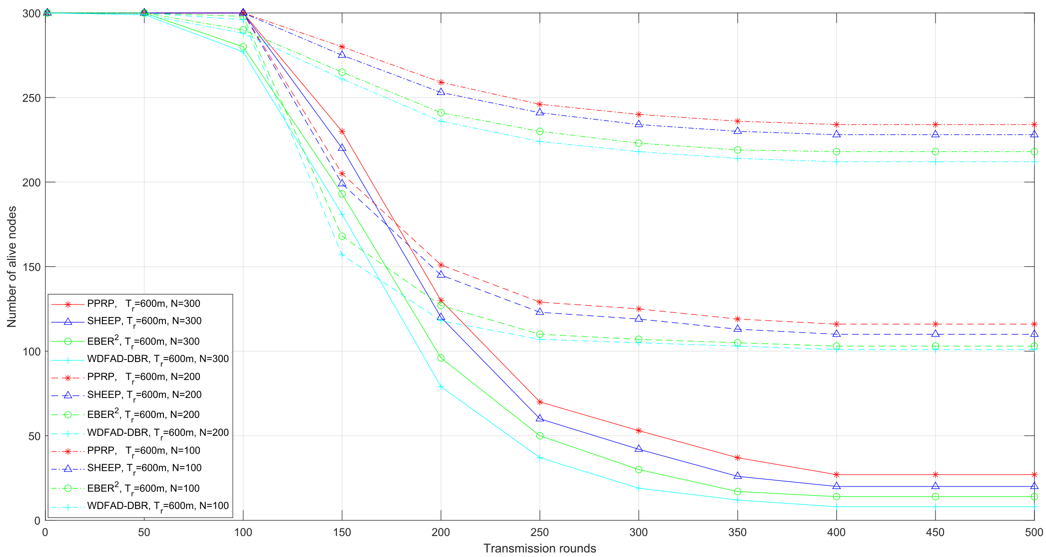

Fig. 15. Alive nodes versus T_{round}, $T_r = 800$ m.

that the more packets transmitted to the base station, the better the E_{Tax} performance. As a result, the proposed PPRP routing protocol has an improved E_{Tax} performance. Table VII supports that the PPRP has better E_{Tax} performance than the SHEEP, EBER^2, and WDFAD-DBR routing protocols, even as T_r grows. Furthermore, the E_{Tax} performance of the PPRP improves with an increase in N irrespective of the T_r as emphasized in Fig 10. Upon closer inspection of Table VIII, it can be seen that the PPRP performs better than the SHEEP, EBER^2, and WDFAD-DBR routing protocols as both N and T_r increase.

D. $PD_{E\text{-}E}$ Performance

The $PD_{E\text{-}E}$ is the amount of time a packet takes to travel from its source node to the base station. This includes the time for transmission, reception and propagation time [5], [32]. Fig. 11 depicts the $PD_{E\text{-}E}$ performance of the PPRP as the network grows in size, assuming $T_{\text{round}} = 100$. The $PD_{E\text{-}E}$ of the PPRP is low in comparison to the SHEEP, EBER^2, and WDFAD-DBR routing protocols for both dense and sparse network. Likewise, irrespective of the value of the T_r, the performance of the PPRP is superior. This is because the proposed PPRP routing protocol considers the T_d in forwarding the packet to the next forwarder and it ensures that the packet is forwarded through the shortest but E-E and E-B path to the base station. Table IX provides more insights into the performance differential between the PPRP and these other routing protocols. For example, at $T_r = 600$ m and $N = 300$, the $PD_{E\text{-}E}$ performance difference between the PPRP and the SHEEP, EBER^2, and WDFAD-DBR routing protocols is 1.0675, 3.1140, and 3.7225 s, respectively. Similarly, as T_r increases to 800 m, the PPRP provides a

$PD_{E\text{-}E}$ performance difference of 0.8978, 2.1898, and 2.5088 s, respectively, demonstrating it as an efficient routing protocol with low latency.

E. Dead/Alive Nodes

The effect of the T_{round} on the network is examined in Figs. 12–15 for $T_r = 600$ m and $T_r = 800$ m. First, as expected in Figs. 12 and 13, the number of dead nodes increase as the T_{round} increases. On the contrary, the number of alive nodes reduce with an increase in the T_{round} as shown in Figs. 14 and 15. Second, the number of dead nodes in Figs. 12 and 13 increase as the network expands in size while the number of alive nodes reduce as depicted in Figs. 14 and 15. More importantly, it can be seen from the figures that the PPRP conserves sensor node battery energy for a longer period than the SHEEP, EBER^2 and WDFAD-DBR routing protocols, regardless of the value of N and T_r. As expected, the proposed PPRP routing protocol conserves the network energy to communicate the sensed information to the nearest sink, resulting in a higher number of alive nodes or a low number of dead nodes after each transmission round as compared to the SHEEP, EBER^2, and WDFAD-DBR routing protocols. Tables X and XI emphasised on the superior PPRP performance for number of dead nodes at different intervals of the T_{round}. In conserving energy, the PPRP avoids void region formation for a longer period, allowing more packets to reach the base station. Thus, the proposed PPRP can serve as a high performance-efficient alternative routing protocol to most existing routing protocols in the literature including the SHEEP, EBER^2 and WDFAD-DBR routing protocols.

VII. Conclusion

This article proposed a simple but efficient routing protocol for large-scale UWSN that can be used in a variety of industrial applications. First, the proposed PPRP ensures a single E-E and E-B path is available from the source node to the sink before a packet is forwarded. Accordingly, there are no packet duplication or retransmission that can lead to packet collision. Second, the proposed routing protocol ensures that a sensor node has sufficient battery energy before it can join the transmission chain. This implies that a sensor node will not die in the process of relaying the sensed information. Thus, it avoids void region formation for a meaningful transmission duration. Third, the proposed PPRP offers an E-E and E-B route to the base station as it considers different routing metrics to select the closest to the optimal path. Thus, it extends the network lifetime of UWSNs for a long duration, which is a major QoS requirement. Above all, this developed PPRP outperforms the existing routing protocol in the literature and it is suitable for real-time industrial applications. Nonetheless, this proposed PPRP has limited performance due to the number of multipath ($\psi = 3$) employed. As a result, future study could increase the number of multipaths while decreasing the computational time complexity. This is because the larger the value of the multipath, the more complex the PPRP, but the better its performance.

References

[1] H. Luo, Y. Chen, K. Wu, and Y. Yang, “A survey of routing protocols for underwater wireless sensor networks,” *IEEE Commun. Surveys Tuts.*, vol. 23, no. 1, pp. 137–160, 1st Quart., 2021.

[2] H. Luo, K. Wu, R. Ruby, Y. Liang, Z. Guo, and L. M. Ni, “Software-defined architectures and technologies for underwater wireless sensor networks,” *IEEE Commun. Surveys Tuts.*, vol. 20, no. 4, pp. 2855–2888, 4th Quart., 2018.

[3] Z. Wadud, A. B. Qazi, F. A. Khan, A. Derhab, I. Ahmad, and M. Ahmad, “An energy balanced efficient and reliable routing protocol for underwater wireless sensor networks,” *IEEE Access*, vol. 7, pp. 175980–175999, 2019.

[4] M. Chaudhary, N. Goyal, A. Benslimane, L. K. Awasthi, A. Alwadain, and A. Singh, “Underwater wireless sensor networks: Enabling technologies for node deployment and data collection challenges,” *IEEE Internet Things J.*, vol. 10, no. 4, pp. 3500–3524, Feb. 2023.

[5] M. Ismail, H. Qadir, F. A. Khan, S. Jan, Z. Wadud, and A. K. Bashir, “A novel routing protocol for underwater wireless sensor networks based on shifted energy efficiency and priority,” *Comput. Commun.*, vol. 210, pp. 147–162, Oct. 2023.

[6] H. Karimi, K. Khamforoosh, and V. Maihami, “Improvement of DBR routing protocol in underwater wireless sensor networks using fuzzy logic and bloom filter,” *PLoS One*, vol. 17, no. 2, pp. 1–20, 2022.

[7] O. O. Ogundile and A. S. Alfa, “A survey on an energy-efficient and energy-balanced routing protocol for wireless sensor networks,” *Sensor*, vol. 17, no. 5, p. 1084, 2017.

[8] H. Yu, N. Yao, T. Wang, G. Li, Z. Gao, and G. Tan, “WDFAD-DBR: Weighting depth and forwarding area division DBR routing protocol for UASNs,” *Ad Hoc Netw.*, vol. 37, pp. 256–282, Feb. 2016.

[9] Z. Wadud, K. Ullah, S. Hussain, X. Yang, and A. B. Qazi, “DOW-PR dolphin and whale pods routing protocol for underwater wireless sensor networks (UWSNs),” *Sensors*, vol. 18, no. 5, p. 1529, 2018.

[10] O. O. Ogundile, M. B. Balogun, O. E. Ijiga, and E. O. Falayi, “Energy-balanced and energy-efficient clustering routing protocol for wireless sensor networks,” *IET Commun.*, vol. 13, no. 10, pp. 1449–1457, 2020.

[11] H. Yan, Z. J. Yan, and J.-H. Cui, “DBR: Depth-based routing for underwater sensor networks,” in *Proc. 7th Int. IFIP-TC6 Netw. Conf. Ad Hoc Sens. Netw., Wireless Netw., Next Gener. Internet*, Singapore, 2008, pp. 5–9.

[12] A. Wahid, S. Lee, H.-J. Jeong, and D. Kim, “Energy-efficient depth-based routing protocol for underwater wireless sensor networks,” in *Advanced Computer Science and Information Technology*, vol. 18. Heidelberg, Germany: Springer Verlag, 2011, pp. 223–234.

[13] M. Ismail et al., “Reliable path selection and opportunistic routing protocol for underwater wireless sensor networks,” *IEEE Access*, vol. 8, pp. 100346–100361, 2020.

[14] C. S. Nandyala, H.-W. Kim, and H.-S. Cho, “QTAR: A *Q*-learning-based topology-aware routing protocol for underwater wireless sensor networks,” *Comput. Netw.*, vol. 222, pp. 1–12, Feb. 2023.

[15] Y. Zhang, Z. Jingru, W. Haiyan, S. Xiaohong, W. Bin, and D. Yuan, “Deep reinforcement learning-based adaptive modulation for underwater acoustic communication with outdated channel state information,” *Remote Sens.*, vol. 14, no. 16, p. 3947, 2022.

[16] K. Saleem, L. Wang, and S. Bharany, “Survey of AI-driven routing protocols in underwater acoustic networks for enhanced communication efficiency,” *Ocean Eng.* vol. 8, no. 1, 2024, Art. no. 119606.

[17] S. Fattah, A. Gani, I. Ahmedy, M. Y. I. Idris, and I. A. T. Hashem, “A survey on underwater wireless sensor networks: Requirements, taxonomy, recent advances, and open research challenges,” *Sensors*, vol. 20, no. 18, p. 5393, 2020.

[18] I. Ahmad, T. Rahman, A. Zeb, I. Khan, M. T. B. Othman, and H. Hamam, “Cooperative energy-efficient routing protocol for underwater wireless sensor networks,” *Sensors*, vol. 22, no. 18, pp. 1–15, 2022.

[19] A. Khan et al., “Routing protocols for underwater wireless sensor networks: Taxonomy, research challenges, routing strategies and future directions,” *Sensors*, vol. 18, no. 5, p. 1619, 2018.

[20] K. Sathish, R. Chinthaginjala, A. Rajesh, W. Kim, J. M. Corchado, and M. Abbas, “Underwater wireless sensor networks with RSSI-based advanced efficiency-driven localization and unprecedented accuracy,” *Sensors*, vol. 23, no. 15, pp. 6973, 2023.

[21] S. Kaveripakam and R. Chinthaginjala, “Energy balanced reliable and effective clustering for underwater wireless sensor networks,” *Alexandria Eng. J.*, vol. 77, pp. 41–62, Aug. 2023.

[22] A. D. Wait, *Sonar for Practicing Engineers*, 3rd ed. San Francisco, CA, USA: Wiley, 2002.

[23] M. Stojanovic, “Optimization of a data link protocol for an underwater acoustic channel,” in *Proc. Oceans Europe*, vol. 1, 2005, pp. 68–73.

[24] L. Stutters, H. Liu, C. Tiltman, and D. J. Brown, "Navigation technologies for autonomous underwater vehicles," *IEEE Trans. Syst., Man, Cybern. C, Appl. Rev.*, vol. 88, no. 4, pp. 581–589, Jul. 2008.

[25] M. Stojanovic and J. Preisig, "Underwater acoustic communication channels: Propagation models and statistical characterization," *IEEE Commun. Surveys Tuts.*, vol. 47, no. 1, pp. 84–89, 1st Quart., 2009.

[26] X. Wei, H. Guo, X. Wang, X. Wang, and M. Qiu, "Reliable data collection techniques in underwater wireless sensor networks: A survey," *IEEE Commun. Surveys Tuts.*, vol. 24, no. 1, pp. 404–431, 1st Quart., 2022.

[27] R. J. Urick, *Principles of Underwater Sound for Engineers.* New York, NY, USA: Tata McGraw-Hill Educ., 1967.

[28] K. V. Mackenzie, "Nine-term equation for sound speed in the oceans," *J. Acoust. Soc. Am.*, vol. 70, no. 3, pp. 807–812, 1981.

[29] M. Stojanovic, "On the relationship between capacity and distance in an underwater acoustic communication channel," *ACM SIGMOBILE Mobile Comput. Commun. Rev.*, vol. 11, no. 4, pp. 34–43, 2007.

[30] S. Climent, A. Sanchez, J. V. Capella, N. Meratnia, and J. J. Serrano, "Underwater acoustic wireless sensor networks: Advances and future trends in physical, MAC and routing layers," *Sensors*, vol. 14, no. 1, pp. 795–833, 2014.

[31] K. Rajakumari, P. Punitha, L. Kumar, and C. Suresh, "Improvising packet delivery and reducing delay ratio in mobile ad hoc network using neighbour coverage-based topology control algorithm," *Int. J. Commun. Syst.*, vol. 35, no. 2, p. e4260, 2022.

[32] K. Saeed et al., "Analyzing the impact of active attack on the performance of the AMCTD protocol in underwater wireless sensor networks," *Sensors*, vol. 23, no. 6, p. 3044, 2023.

Olayinka O. Ogundile (Member, IEEE) received the B.Eng. degree in electrical engineering from the University of Ilorin, Ilorin, Nigeria, in 2007, the M.Sc. degree in communication engineering from The University of Manchester, Manchester, U.K., in 2010, and the Ph.D. degree from the University of the Witwatersrand, Johannesburg, South Africa, in 2016.

He is currently a Senior Lecturer with the Department of Industrial Technical Education (Electrical/Electronic), Tai Solarin University of Education, Ijebu Ode, Nigeria. He is also an Extraordinary Senior Lecturer with the Department of Electrical and Information Engineering, Stellenbosch University, Stellenbosch, South Africa. He was a Postdoctoral Research Fellow with the School of Electrical and Information Engineering, University of the Witwatersrand, in 20l6, also with the Department of Electrical, Electronic and Computer Engineering, University of Pretoria, Pretoria, South Africa, from 2016 to 2017, and also with the Department of Electrical and Information Engineering, Stellenbosch University from 2019 to 2021. His research interests include digital communication, digital transmission techniques, digital signal processing/machine learning, channel estimation, forward error correction, and wireless sensor networks.

Oluwaseyi P. Babalola (Senior Member, IEEE) received the B.Sc. degree in mathematics (Hons.) from the University of Ibadan, Ibadan, Nigeria, in 2009, the M.Sc. (Eng.) degree in electrical engineering from the University of the Witwatersrand, Johannesburg, South Africa, in 2017, and the Ph.D. degree in electronic engineering from Stellenbosch University, Stellenbosch, South Africa, in 2020.

He is currently a Lecturer and a Member with the French South African Institute of Technology and the African Space Innovation Centre with the Department of Electrical, Electronic, and Computer Engineering, Cape Peninsula University of Technology, Cape Town, South Africa. He is the Project Leader of the Ocean Plastics and Composites Project within FSATI CPUT. He has published widely and is a reviewer for several journals and conferences. His research interests include advanced error-correcting coding, digital signal processing techniques, and artificial intelligence with applications to visible light communications, wireless communications, underwater acoustic communications, storage systems, and ocean plastics.

Dr. Babalola is a recipient of several grants and awards, including the CPUT Research Award 2023. He is a volunteer for various societies, committees, and groups. He is a Y2-Rated Researcher from the National Research Foundation, in South Africa.

Emmanuel O. Agboola received the B.Sc. degree in computer science from Ajayi Crowther University, Oyo, Nigeria, in 2012, the first master's degree in information technology from Ladoke Akintola University of Technology, Ogbomosho, Nigeria, in 2017, and the second master's degree in Internet of Things with cybersecurity from Bournemouth University, Poole, Dorset, U.K., in 2024.

He was with HIQOS Technologies Ltd., Lagos, Nigeria, in several designation, such as a Site Collection Administrator (Share point), a Network Security Engineer, a Cloud Solutions Architect, and a Lead Information Technology Infrastructure Analyst. He is Currently a Cloud Security Engineer (Part time) with Cybarik Ltd., Essex, U.K. His core competencies are in security architecture and technologies, routing and switching technologies, network security, cloud security architecture, IP address structuring, Windows and Linux OS, Internet of Things, and cyber security with expertise in threat detection, Identity management, and security framework implementation.

Olabisi M. Ogundile received the B.Sc. degree in computer science from the Tai Solarin University of Education, Ijebu Ode, Nigeria, in 2014, where she is currently pursuing the master's degree with the Department of Computer Science.

She is currently a Level 9 Officer with the Government Senior College, Ketu-Epe, Nigeria. Her research interests are in IoT, machine learning, and artificial intelligence.

Innocent E. Davidson (Senior Member, IEEE) received the B.Sc. (Eng.) (Hons.) and M.Sc. (Eng.) degrees in electrical engineering from the University of Ilorin, Ilorin, Nigeria, in 1984 and 1987, respectively, the Ph.D. degree in electrical engineering from the University of Cape Town, Cape Town, South Africa, in 1998, and the PG diploma degree in business management from the University of KwaZulu-Natal, Durban, South Africa, in 2004.

He is a Full Professor and a Director with the French South African Institute of Technology, and the African Space Innovation Center, Cape Peninsula University of Technology. He has supervised six postdoctoral research fellows and graduated 66 Ph.D./masters' students and over 1200 engineers, technologists, and technicians. He is the author/co-author of 405 technical papers in accredited journals, and peer-reviewed conference proceedings and book chapters. He has managed over U.S. \$3.5 million in research funds. His current research interests include Space and CNS Innovation, smart grids, electromagnetics, and applied artificial intelligence.

Prof. Davidson is a recipient of numerous international Best Paper Awards. He also received the Associate Certificate in Sustainable Energy Management from the British Columbia Institute of Technology, Burnaby, BC, Canada, in 2011, and the Course Certificate in Artificial Intelligence from the University of California at Berkeley, USA, in 2020. He is a Fellow Grade of the Institute of Engineering and Technology, U.K., and the South African Institute of Electrical Engineers, a Chartered Engineer in the U.K., and a Registered Professional Engineer of the Engineering Council of South Africa. He is a member of the Western Canada Group of Chartered Engineers, the Institute of Engineering and Technology (IET Canada) British Columbia Chapter, IEEE Collabratec Communities on Smart Cities and IEEE (South Africa Chapter). He is a C2-Rated researcher from the National Research Foundation, South Africa.